



MRI features in 17 patients with L2 hydroxyglutaric aciduria

Héla Fourati^{a,b,*}, Emna Ellouze^{b,c}, Mourad Ahmadi^a, Dhouha Chaari^b, Fatma Kamoun^{b,c}, Ines Hsairi^{b,c}, Chahnez Triki^{b,c}, Zeineb Mnif^{b,c}

^a Radiology Departement Hedi Chaker Hospital, EL Ain Road, 3002 3089 Sfax, Tunisia

^b Neuropediary Reaserch Unit (UR12ES16), Faculty of Medecine at Sfax university Tunisia, Boulevard Majida Boulila 3089 Sfax Tunisia

^c Pediatric Neurology department Hedi Chaker Hospital, EL Ain Road, 3089 Sfax, Tunisia

ARTICLE INFO

Article history:

Received 21 July 2016

Received in revised form 30 August 2016

Accepted 24 September 2016

Available online 27 September 2016

Keywords:

L-2-Hydroxyglutaric aciduria

Leukoencephalopathy

MRI

Spectroscopy

ABSTRACT

L-2-Hydroxyglutaric (L-2-HG) aciduria is a rare inherited metabolic disease usually observed in children. Patients present a very slowly progressive deterioration with cerebellar ataxia, mild or severe mental retardation, and various other clinical signs including extrapyramidal and pyramidal symptoms, and seizures Goffette et al. [1]. This leukoencephalopathy was first described in 1980 Duran et al. [2]. Brain magnetic resonance imaging (MRI) demonstrates nonspecific subcortical white matter (WM) loss, cerebellar atrophy and changes in dentate nuclei and putamen Steenweg et al. [3]. The diagnosis is highlighted by increased levels of L-2-HG in body fluids such as urine and cerebrospinal fluid.

The purpose of this study is to retrospectively describe the brain MRI features in L-2-HG aciduria.

© 2016 Published by Elsevier Ltd. This is an open access article under the CC BY-NC-ND license (<http://creativecommons.org/licenses/by-nc-nd/4.0/>).

1. Introduction

L-2-Hydroxyglutaric (L-2-HG) aciduria is a rare recessive autosomal inherited metabolic disease usually observed in children. Patients present a very slowly progressive deterioration with cerebellar ataxia, mild or severe mental retardation, and various other clinical signs including extrapyramidal and pyramidal symptoms, and seizures [1]. This leukoencephalopathy was first described in 1980 [2]. To date, there are a little above one hundred documented cases in medical literature [2–4]. Most are published in case-report form. Steenweg publishes the largest series in 2009 [5]. Neuro imaging findings generally show subcortical leukoencephalopathy, cerebellar atrophy and changes in dentate nuclei and putamen [3,6]. Increased levels of L-2-HG in body fluids such as urine and cerebrospinal fluid or mutational analysis highlight the diagnosis by molecular biology.

The purpose of this study is to retrospectively describe the brain magnetic resonance (MR) abnormalities in patients with L-2-HG aciduria and to identify some features in our series.

2. Case series

2.1. Patients and methods

During a three-year period (between March 1st, 2011, and March 1st, 2014), 17 patients (age range: 3–28 years; median age, 11,6 years) (Table 1) with a clinical suspicion of (L-2-HG) aciduria disease underwent brain MRI examination, including, in five cases, proton MR spectroscopy.

Patients underwent MRI within a 35,6-day period, (period range, 1–120 days; median period 30 days) after the outset of the first clinical abnormality. All patients were followed in the pediatric neurology Department.

Meanwhile, the clinical suspicion was confirmed by the increased levels of L-2-HG in body fluids and by molecular biology.

Brain MRI examinations were performed with a 1.5-T MR imaging system with a head coil. All our patients underwent general anaesthesia or mild sedation in order to perform MRI examination. The sedation was necessary because of the mental retardation in all the patients.

The protocol (Table 2) included sagittal T1 weighted images, axial and coronal T2 weighted Fast Spin Echo (FSE) sequences in all cases, T2 FLAIR (fluid attenuated inversion recovery) weighted images in almost half of the cases (47%) and diffusion-weighted images (DWI) in only three cases (17,6%).

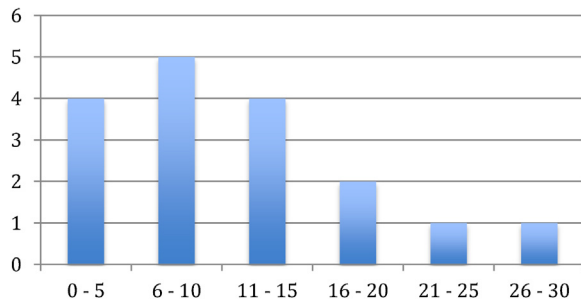
Abbreviations: L-2-HG, L-2-Hydroxyglutaric; MRI, Magnetic resonance imaging; WM, white matter; WMA, white matter abnormalities; GM, Gray matter.

* Corresponding author at: Radiology department, Hedi Chaker Hospital, EL Ain Road, Sfax 3002 3089, Tunisia.

E-mail addresses: fourati_hela@yahoo.fr, fouratihela15@gmail.com (H. Fourati).

<http://dx.doi.org/10.1016/j.ejro.2016.09.001>

2352-0477/© 2016 Published by Elsevier Ltd. This is an open access article under the CC BY-NC-ND license (<http://creativecommons.org/licenses/by-nc-nd/4.0/>).

Table 1
Patient's distribution by age group.

Monovoxel spectroscopy was added in the protocol in five patients (both long TE and short TE in three cases and only long TE in 2 patients).

A contrast agent was administered in one patient who have an associated cerebral hematoma to determine the underlying cause. The patients did not receive the same MR protocol because the MR images were collected for three centers, but all the patients were all followed in the pediatric neurology department in our hospital, which is, specialized, inter alia, in metabolic diseases. Two radiologists, 5 and 15 years of experience with pediatric MR image interpretation respectively, performed retrospectively the analysis of the available images. A consensus reading was performed. The radiologists were informed about the diagnosis but blinded to clinical condition.

This analysis was based on the collection of some items systematically for each patient according to a pre-established reading grid (Table 3). The predominant location of the abnormalities was precised.

For the location of the White matter abnormalities (WMA), the readers noted the involvement of the subcortical WM, the periventricular WM and the central WM. WM swelling was defined as increased volume leading to broadening of gyri; WM rarefaction was defined as T2-hyperintense WM areas with low signal intensity on FLAIR images, but not as low as the signal intensity of cerebrospinal fluid [3].

For the basal ganglia was noted the presence of an outer rim sign defined by a more prominent signal intensity in the periphery.

3. Results

White matter MR abnormalities which are consisting of either swelling or rarefaction were present in the frontal and temporal lobes of the brain in all cases (Fig. 1). Parietal and occipital abnormalities were present in 94% and 88% respectively. WM abnormalities were most severe in the frontal regions (82,3%) (Graph1).

Subcortical abnormalities were present in most cases, representing the predominantly involved area (82,3%), followed by central WM (11,7%) and than periventricular WM (5,9%).

Table 2
MR protocol.

Sequence	Plan	Field Of View (cm)	Echo Time (ms)	Repetition Time (ms)	Flip Angle	Section thickness (mm)	Acquisition time (s)
SE T1	Sagittal	24	20	640	90°	5	163
FSE T2	Axial	24	119,3	5400	90°	5	81
FSE T2	Coronal	24	119,3	5400	90°	5	81
FLAIR ^a	Axial	24	114	9502	90°	5	190
Diffusion(b0, b1000)	Axial	24	98,7	6000		5	54
T1 SPGR ^b	3D	24	4	9,2	90°	1,4	144

^a Fluid Attenuated Inversion recovery.

^b spoiled gradient.

Table 3
MR abnormalities reading grid.

WM* Structures	Lobes	Yes/No; location
	Frontal WM	
	Temporal WM	
	Parietal WM	
	Occipital WM	
	Predominantly involved lobe	
	Subdivison	
	Predominantly involved zone	
	Other structures	
	Corpus callosum	
	Extreme/External capsule	
	Internal capsule involved	
	Cerebellar WM	
	Cerebellar peduncles	
	Brainstem	
WMA**	Symmetry	
	WM Swelling	
	Predominant location of swollen WM	
	WM rarefaction	
	Cysts	
GM*** Structures	Cerebral cortex	
	Thalamus	
	Globus pallidus	
	Caudate nucleus	
	Putamen	
	Dentate nucleus	
	Cerebellar cortex	
Atrophy	Cerebral atrophy	
	Cerebellar atrophy (vermis/hemispheres)	

WM: White matter; WMA**: White matter abnormalities; GM***: Gray matter.

Extreme and external capsules were affected in 9 patients (52,9%). Internal capsule was affected in only two cases (Fig. 2). Internal and external capsules were both spared in 41,2% of cases. Corpus callosum and cerebellar WM were spared in all cases. Brainstem was affected in only one patient (5,9%).

WM abnormalities were bilaterally symmetrical in all the patients. These WM abnormalities were confluent in 12 patients.

Affected WM swelling was seen in 13 patients (76,5%), involving more frequently frontal (76,5%) and temporal (64,7%) lobes. Occipital lobe was spared in all cases. Among affected areas, predominant swollen WM was seen in frontal lobe in 11 patients (84,6%) (Fig. 3).

Atrophy of cerebral WM was found in 47,1% of our patients. Cerebellar vermis atrophy was found in 11,8%, and cerebellar hemispheres in only one patient.

In 2 of 17 patients, there were cystic changes involving the frontal lobe in one case and the dentate nucleus in the other. In one case the readers noted a WM rarefaction involving the temporal lobe (Fig. 4).

Cerebral cortex was involved in only one case (temporal lobe), while none of our patients had cerebellar cortex abnormalities.

The dentate nucleus was affected in all patients (Fig. 5). Other nuclei were variably affected, the caudate nucleus in 6 patients (35,3%), the putamen in 12 patients (70,6%), the globus pallidus in

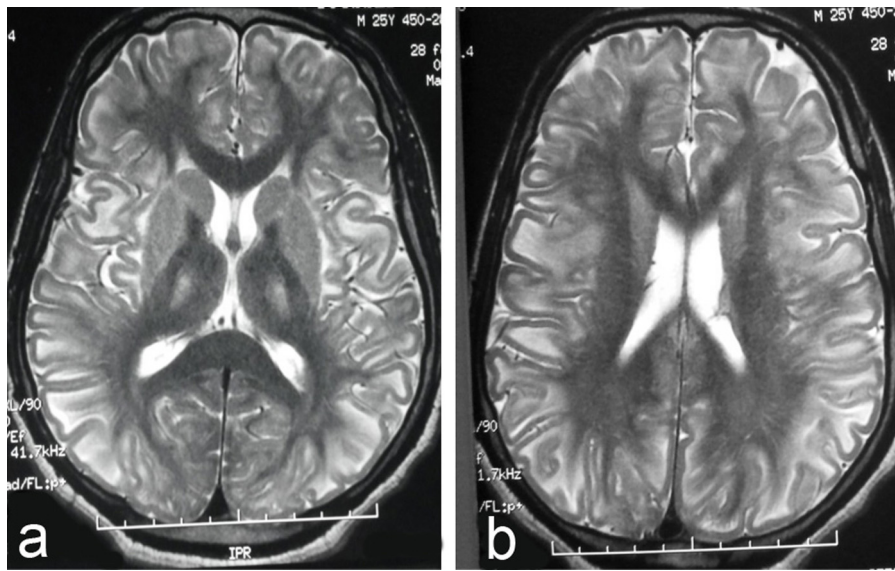


Fig. 1. Axial T2 FSE weighted images showing signal abnormalities: “swelling” affecting subcortical white matter (WM) (a, b) in almost all cerebral areas, with a slight parieto-temporal predominance. External capsula and both of the thalami (a) are also affected.

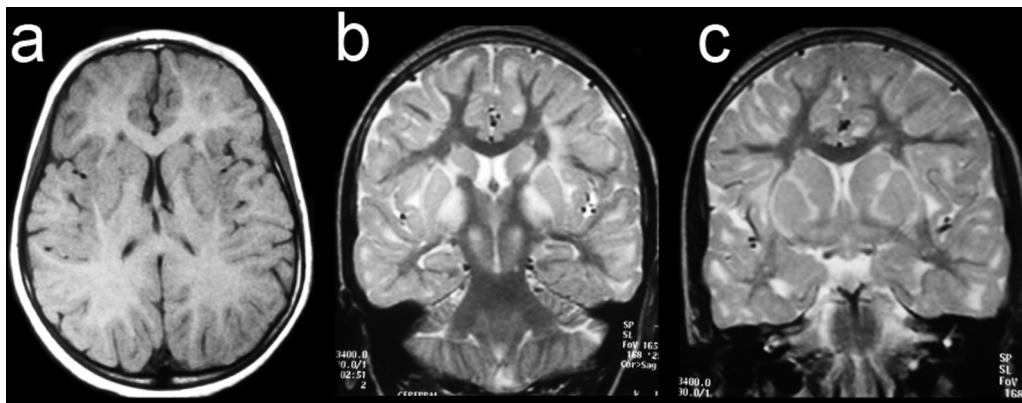


Fig. 2. Axial T1 SE weighted image (a), and coronal T2 FSE weighted images (b and c) showing extensive WM abnormalities, affecting outer and inner capsula with mesencephalic abnormalities. An outer rim sign can also be noted for the putamen.

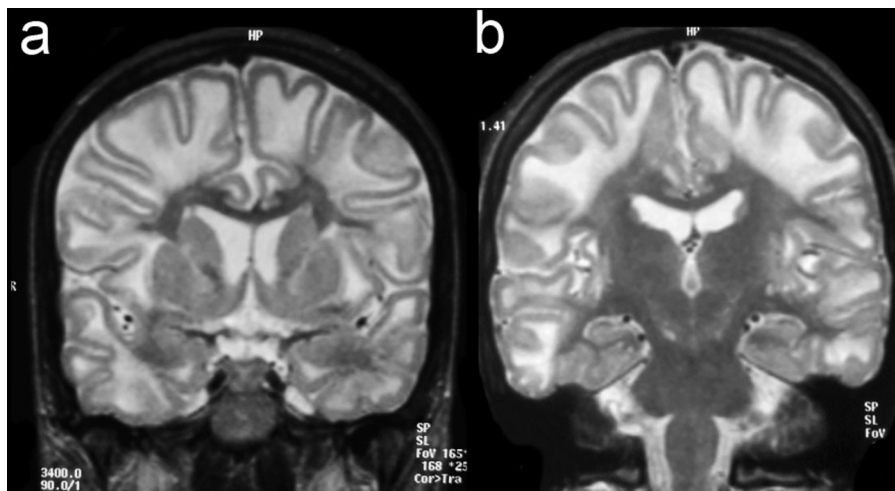


Fig. 3. Coronal T2 FSE weighted images showing WM abnormalities involving subcortical, central and periventricular areas with swollen WM appearance. An outer rim sign, outer and inner capsula involvements are also present.

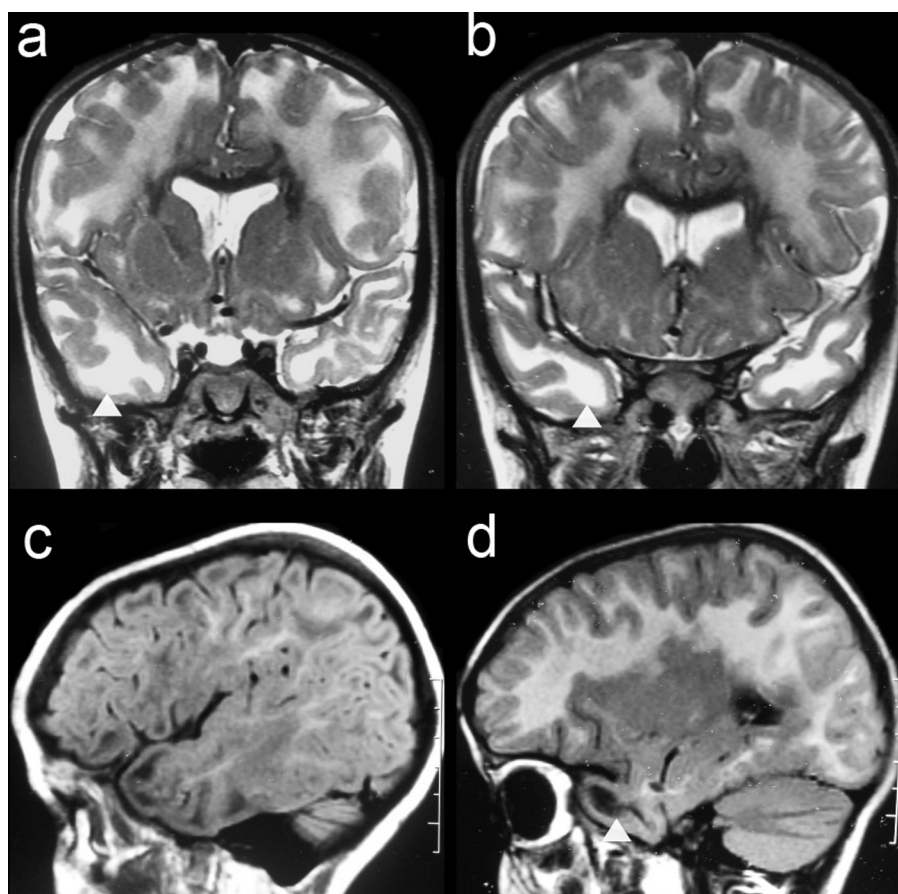


Fig. 4. Coronal T2 FSE weighted images (a and b) and sagittal T2 FLAIR weighted images (c and d), showing WM abnormalities with WM swelling in frontal lobes (a and b), some of signal abnormalities present a hyposignal in T2 FLAIR sequence (figures c and d: WM rarefaction).

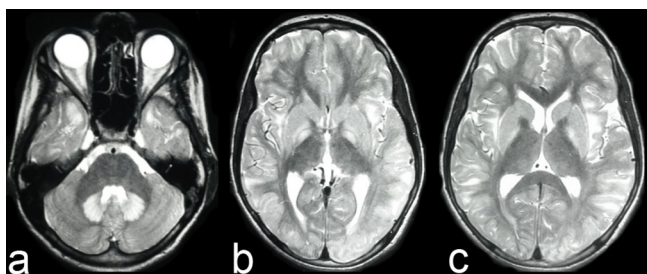


Fig. 5. Axial T2 FSE weighted images showing the involvement of the dentate nucleus (a), the globus pallidus (b). An outer rim sign is observed (c).

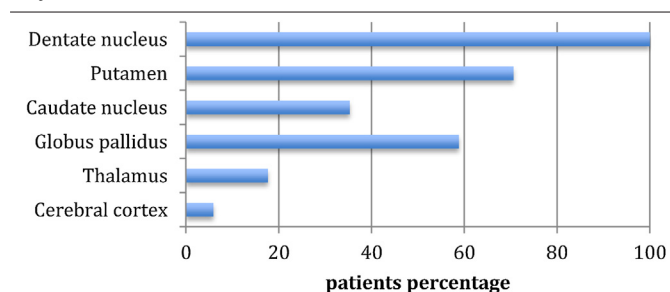
10 patients (58,8%) and the thalamus in only 3 cases (17,6%). Three out of the 6 cases where caudate nucleus was involved presented an outer rim sign in the T2-weighted images, as well as 7 from the 12 patients who had putaminal abnormalities.

Gray matter (GM) structures involvement was summarized in the table below (Table 4).

Monovoxel magnetic resonance spectroscopy (MRS) was performed in 5 patients. In one patient MRS was normal. It has revealed decrease in NAA, and choline peaks (Fig. 6) in four cases and multiplet 2,2 –2,7 in one case.

We tried, also, to determine what correlations exist between the clinical presentation (severity of the clinical presentation and the disease's duration) and the MR parameters in collaboration with the neuro-paediatrists. The MRI of patients belonging to the same family were compared in order to give some specificities.

Table 4
Gray matter MR abnormalities.



No statistical correlation can be established because of the small number of patients in each family, but we think that the severity of MR parameters is correlated to the severity of clinical presentation rather than to the disease duration. However, the white matter atrophy can be correlated to the disease duration. Moreover, we found no imaging particularity correlated to the family affiliation. The Fig. 7 illustrate MR features in two patients belonging to the same family. The first patient is 17 years old, the disease duration for him is 16 years, he had severe clinical presentation with psychomotor delay, moderate mental retardation, tremors, epilepsy, pyramidal syndrome, chorea and rigidity, cerebellar syndrome. The patient is 35 years old, the disease duration is 34 years, he had mild clinical presentation with psychomotor delay, mild mental retardation, epilepsy, pyramidal syndrome, cerebellar syndrome, no chorea and rigidity, no tremors

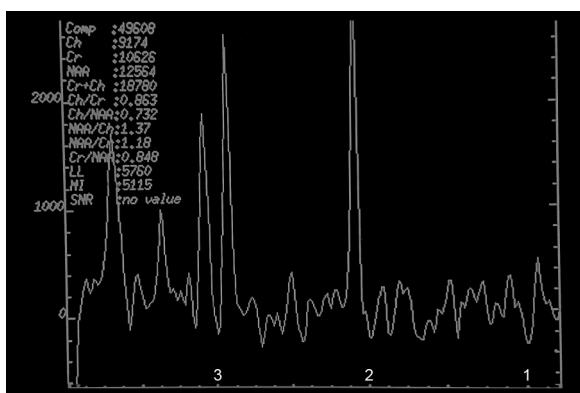


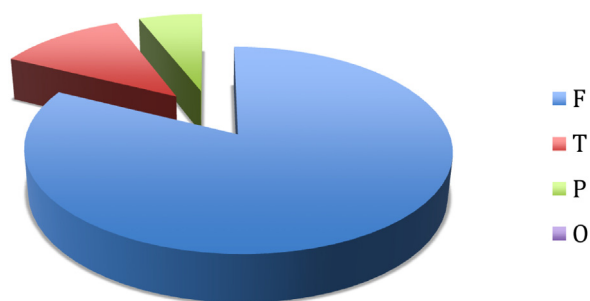
Fig. 6. Monovoxel spectroscopy on frontal WM abnormalities shows decrease of NAA and Choline peaks.

4. Discussion

L-2-Hydroxyglutaric aciduria occurs in both sexes. Symptoms usually appear in early childhood [1]. The diagnosis is supported by increased levels of L-2-HG acid in urine, plasma, and cerebro-spinal fluid [5] or by genetic analysis.

A close correlation between the clinical disability and the extent of pathologic changes on MRI has been reported [7]. The combination of sub-cortical leukoencephalopathy sparing the deep white matter and the corpus callosum together with atrophy of the cerebellar vermis and involvement of both dentate nuclei has been considered pathognomonic for L-2-HG aciduria [3]. Our results concur with the literature: the most affected areas are subcortical frontal WM and all of our patients had abnormalities in dentate nuclei. The dentate nucleus and putamen are constantly affected in many series, whereas, globus pallidus and caudate nucleus were variably affected. In our patients, we observed putamen involvement in 71% of cases. Thalamus and brain stem sparing is a characteristic clue for differentiating L-2-HG aciduria from Canavan's disease in patients with macrocephaly and diffuse leukoencephalopathy [8,9]. One of our patients had a brainstem abnormal signal and in three cases we reported thalamic anomalies.

There are a few descriptions of histologic brain findings in L2-HG aciduria. They reported WM abnormalities (spongiosis, demyelination and cystic degeneration) most pronounced in sub-cortical regions [10].



Graph 1. Predominantly involved lobe in White matter MR abnormalities.

Some studies have been reported, in which the authors describe malignant brain tumors of variable nature, during the course of the disease [6,11–13].

None of our patients had a brain tumor.

Few data on proton MR spectroscopic changes are available. Decreased NAA and choline peaks, together with an increase in the *myo*-inositol peak, were reported [13]. L-2-HG acid is also known to generate three multiplets centered, respectively, at 1.91, 2.03, and 2.43 ppm [1]. An unusual singlet at 2.5 ppm has been recently described using the multivoxel PRESS technique in another patient [1]. A multiplet at 2.10–2.50 ppm might be seen, and could be generated by elevated glutamate and glutamine or L-2-hydroxyglutaric acid itself, which has a similar chemical structure to glutamate [14].

We observed using the mono-voxel STEAM technique in four of our patients a decrease in NAA and Choline peaks and a multiplet 2.20–2.70 in one patient. The validity of identification of an unusual peak on proton MR has been documented in other metabolic diseases. However, no specific peaks have yet been clearly described for HG acid [15].

Our study had several limitations due to its small number of patients. Another limitation may be the retrospective nature of our study and the small number of patients in whom we practiced magnetic resonance spectroscopy.

In the future, further studies investigating MRS findings may determine its role in the diagnosis and possibly in the staging of the severity of the disease.

In conclusion, MRI in L2HGA permit to find morphological changes involving particular areas. This study shows consistent results with the literature.

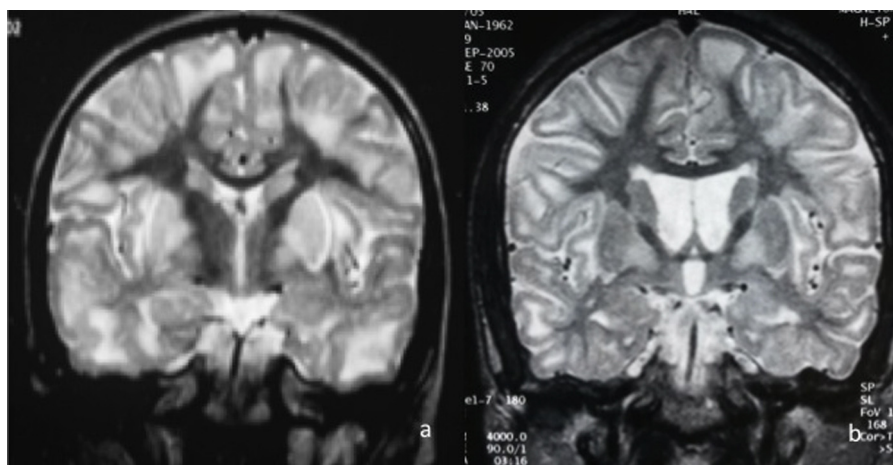


Fig. 7. The comparison of the two coronal T2 slices in patient a and b show that in « a » there is obvious white matter signal abnormality (in fronto-temporal), basal ganglia involvement, these features are more pronounced in « b ». We also note the ventricles' enlargement in b (not present in a) due to white matter atrophy.

Further studies with larger populations are needed to help the clinical management of patients with inherited neurometabolic disorders.

Competing interest

The authors declare that there is no competing interest.

Acknowledgements

1. Service de Neurologie Pédiatrique, C.H.U Hédi Chaker de Sfax, Sfax, Tunisia 2. Laboratoire de Génétique Moléculaire Humaine, Faculté de Médecine de Sfax, Université de Sfax, Sfax, Tunisia; 3. UR/08-08, département de biochimie, hopital Rabta, Tunis, Tunisie.

References

- [1] S.M. Goffette, T.P. Duprez, M.-C.L. Nassogne, M.-F.A. Vincent, C. Jakobs, C.J. Sindic, L-2-Hydroxyglutaric aciduria: clinical, genetic, and brain MRI characteristics in two adult sisters, *Eur. J. Neurol.* 13 (5) (2006) 499–504.
- [2] M. Duran, J.P. Kamerling, H.D. Bakker, A.H. van Gennip, S.K. Wadman, L-2-Hydroxyglutaric aciduria: an inborn error of metabolism? *J. Inherit. Metab. Dis.* 3 (4) (1980) 109–112.
- [3] M.E. Steenweg, G.S. Salomons, Z. Yapici, G. Uziel, E. Scalais, D.I. Zafeiriou, et al., L-2-Hydroxyglutaric aciduria: pattern of MR imaging abnormalities in 56 patients 1, *Radiology* 251 (3) (2009) 856–865.
- [4] A. Larnaout, F. Hentati, S. Belal, C. Ben Hamida, N. Kaabachi, M. Ben Hamida, Clinical and pathological study of three Tunisian siblings with L-2-hydroxyglutaric aciduria, *Acta Neuropathol.* 88 (4) (1994) 367–370.
- [5] P.G. Barth, G.F. Hoffmann, J. Jaeken, W. Lehnert, F. Hanefeld, A.H. van Gennip, et al., L-2-Hydroxyglutaric acidemia: a novel inherited neurometabolic disease, *Ann. Neurol.* 32 (July (1)) (1992) 66–71.
- [6] F. London, Gliomatosis cerebri in L-2-hydroxyglutaric aciduria, *Acta Neurol. Belg.* 115 (December (4)) (2015) 749–751.
- [7] I. Moroni, L. D'Incerti, L. Farina, M. Rimoldi, G. Uziel, Clinical, biochemical and neuroradiological findings in L-2-hydroxyglutaric aciduria, *Neurol Sci.* 21 (April (2)) (2000) 103–108.
- [8] M. Topçu, G. Erdem, I. Saatçi, G. Aktan, A. Simşek, Y. Renda, et al., Clinical and magnetic resonance imaging features of L-2-hydroxyglutaric acidemia: report of three cases in comparison with Canavan disease, *J. Child Neurol.* 11 (September (5)) (1996) 373–377.
- [9] D.I. Zafeiriou, W.J. Kleijer, G. Maroupoulos, A.L. Anastasiou, P. Augoustidou-Savvopoulou, F. Papadopoulou, et al., Protracted course of N-acetylaspartic aciduria in two non-Jewish siblings: identical clinical and magnetic resonance imaging findings, *Brain Dev.* 21 (April (3)) (1999) 205–208.
- [10] C. Barbot, I. Fineza, L. Diogo, M. Maia, J. Melo, A. Guimarães, et al., L-2-Hydroxyglutaric aciduria: clinical, biochemical and magnetic resonance imaging in six Portuguese pediatric patients, *Brain Dev.* 19 (July (4)) (1997) 268–273.
- [11] P.A. Ozişik, N. Akalan, S. Palaoğlu, M. Topçu, Medulloblastoma in a child with the metabolic disease L-2-hydroxyglutaric aciduria, *Pediatr. Neurosurg.* 37 (July (1)) (2002) 22–26.
- [12] Patay Zoltan, Brent A. Orr, Barry L. Shulkin, Scott N. Hwang, Yuan Ying, Alberto Broniscer, Frederick A. Boop, David W. Ellison, Successive distinct high-grade gliomas in L-2-hydroxyglutaric aciduria, *J. Inherit. Metab. Dis.* 38 (March (2)) (2015) 273–277.
- [13] S. Kurul, H. Cakmakçi, E. Dirik, Glutaric aciduria type 1: proton magnetic resonance spectroscopy findings, *Pediatr. Neurol.* 31 (September (3)) (2004) 228–231.
- [14] K. Aydın, M. Ozmen, B. Tatli, S. Sencer, Single-voxel MR spectroscopy and diffusion-weighted MRI in two patients with L-2-hydroxyglutaric aciduria, *Pediatr. Radiol.* 33 (December (12)) (2003) 872–886.
- [15] R.N. Sener, L-2 Hydroxyglutaric aciduria: proton magnetic resonance spectroscopy and diffusion magnetic resonance imaging findings, *J. Comput. Assist. Tomogr.* 27 (January/ February (1)) (2003) 38–43.